

# Seismic Modeling: Discrete Grid Methods

Wednesday Morning, September 26th

## Wave Propagation in the Vicinity of a Cylindrical Object

SD1.1

David Kessler\* and Dan Kosloff, Tel Aviv University, Israel

### Summary

Wave propagation in the vicinity of cylindrical objects is a problem which appears in many branches of physics and engineering. In particular, in the area of Geophysics there are many problems which include the presence of a cylindrical borehole. Unfortunately, closed form solutions for such problems exist only for the most simple configurations. Therefore, presence of material variability as in the earth, one needs to resort to numerical solution techniques. However, use of methods such as finite differences, finite elements or pseudospectral methods in cartesian geometry will usually not be successful due to the small size of the borehole (on the order of 20 cm) compared to the distance which the waves propagate (often on the order of few kilometers). In addition the representation of a cylindrical object on a rectangular mesh causes spurious diffractions.

In this work we present a spectral technique for solving the two dimensional acoustic and elastic wave propagation problems in the presence of cylindrical objects. The method is based on spatial discretization of the solution in a cylindrical  $(r, \theta)$  coordinate system where  $r$  is the distance from the center of the numerical mesh and  $\theta$  is the radial angle. The solution is approximated by a Chebychev expansion in the  $r$  direction which results in non-uniform grid spacing (Figure 1). The fine grid spacing in the center of the mesh has the advantage of allowing many grid points to cover a very small physical space in that region. The Chebychev expansion also allows to treat the absorbing boundary conditions at the edges of the grid. For the azimuthal angle coordinate, we use the periodic Fourier expansion.

### Equations of Motion for an Acoustic Medium

The numerical algorithm for the acoustic case is based on the solution of the acoustic wave equation for constant density in two dimensional cylindrical coordinates  $(r, \theta)$  given by,

$$\frac{1}{r} \frac{\partial}{\partial r} \left[ r \frac{\partial P}{\partial r} \right] + \frac{1}{r^2} \frac{\partial^2 P}{\partial \theta^2} + S = \frac{1}{c^2} \frac{\partial^2 P}{\partial t^2} \quad (1)$$

where  $r$  is the radius,  $\theta$  is the radial angle,  $P$  is the pressure field,  $S$  is the source term and  $t$  denotes time. For the numerical algorithm, we recast (1) as a system of three coupled first order equations given by:

$$\frac{\partial}{\partial t} \begin{bmatrix} \dot{P} \\ r \frac{\partial P}{\partial r} \\ \frac{\partial P}{\partial \theta} \end{bmatrix} = \mathbf{A} \begin{bmatrix} \dot{P} \\ r \frac{\partial P}{\partial r} \\ \frac{\partial P}{\partial \theta} \end{bmatrix} + \mathbf{B} \begin{bmatrix} \dot{P} \\ r \frac{\partial P}{\partial r} \\ \frac{\partial P}{\partial \theta} \end{bmatrix} + \begin{bmatrix} S \\ 0 \\ 0 \end{bmatrix} \quad (2)$$

where

$$\mathbf{A} = \begin{bmatrix} 0 & \frac{c^2}{r} & 0 \\ r & 0 & 0 \\ 0 & 0 & 0 \end{bmatrix} \quad \text{and} \quad \mathbf{B} = \begin{bmatrix} 0 & 0 & \frac{c^2}{r^2} \\ 0 & 0 & 0 \\ 1 & 0 & 0 \end{bmatrix} \quad (3)$$

The numerical algorithm solves equation (2) with appropriate boundary condition at  $r = a$  and at  $r = b$ .

### Equations of motion for an Elastic Medium

The numerical algorithm for the elastic case is based on a solution of the equations of conservation of momentum combined with the stress-strain relation for an isotropic elastic solid undergoing infinitesimal deformation. For two dimensional cylindrical coordinates  $(r, \theta)$  the equations of momentum conservation are given by:

$$\rho \ddot{U}_r = \frac{1}{r} \frac{\partial}{\partial r} \left[ r \sigma_{rr} \right] + \frac{1}{r} \frac{\partial \sigma_{r\theta}}{\partial \theta} - \frac{\sigma_{\theta\theta}}{r} + f_r \quad (4)$$

$$\rho \ddot{U}_\theta = \frac{1}{r^2} \left[ r^2 \sigma_{r\theta} \right] + \frac{1}{r} \frac{\partial \sigma_{\theta\theta}}{\partial \theta} + f_\theta$$

(Fung, 1965). where  $U_r$  and  $U_\theta$  are the  $r$  direction and  $\theta$  direction displacements,  $\sigma_{rr}$ ,  $\sigma_{\theta\theta}$  and  $\sigma_{r\theta}$  are the stress components,  $f_r$  and  $f_\theta$  are body forces per unit volume, and  $\rho$  denotes the density.

The stress-strain relation for an isotropic elastic solid expressed in terms of displacement derivatives in cylindrical coordinate reads:

$$\sigma_{rr} = \left[ \lambda + 2\mu \right] \frac{\partial U_r}{\partial r} + \frac{\lambda}{r} U_r + \frac{\lambda}{r} \frac{\partial U_\theta}{\partial \theta} \quad (5)$$

$$\sigma_{\theta\theta} = \left[ \lambda + 2\mu \right] \frac{U_r}{r} + \frac{\lambda + 2\mu}{r} \frac{\partial U_\theta}{\partial \theta} + \lambda \frac{\partial U_r}{\partial r}$$

$$\sigma_{r\theta} = \frac{\lambda}{r} \frac{\partial U_r}{\partial \theta} + \mu \frac{\partial U_\theta}{\partial r} - \frac{\mu}{r} U_\theta$$

where  $\lambda$  and  $\mu$  are respectively the rigidity and the shear modulus.

For the numerical algorithm described in this study equations (4) and (5) are recast as a system of five coupled first order equations given by:

$$\frac{\partial}{\partial t} \begin{bmatrix} \dot{U}_r \\ \dot{U}_\theta \\ \sigma_{rr} \\ \sigma_{\theta\theta} \\ \sigma_{r\theta} \end{bmatrix} = \mathbf{A} \begin{bmatrix} \dot{U}_r \\ \dot{U}_\theta \\ \sigma_{rr} \\ \sigma_{\theta\theta} \\ \sigma_{r\theta} \end{bmatrix} + \mathbf{B} \begin{bmatrix} \dot{U}_r \\ \dot{U}_\theta \\ \sigma_{rr} \\ \sigma_{\theta\theta} \\ \sigma_{r\theta} \end{bmatrix} + \begin{bmatrix} \frac{\sigma_{rr} - \sigma_{\theta\theta}}{\rho r} \\ \frac{2\sigma_{r\theta}}{\rho r} / (\rho r) \\ (\lambda/r) \dot{U}_r \\ (\lambda + 2\mu)/r \dot{U}_r \\ -\frac{\mu}{r} \dot{U}_\theta \end{bmatrix} + \begin{bmatrix} (f_r)/\rho \\ (f_\theta)/\rho \\ 0 \\ 0 \\ 0 \end{bmatrix} \quad (6)$$

where

$$\mathbf{A} = \begin{bmatrix} 0 & 0 & 1/\rho & 0 & 0 \\ 0 & 0 & 0 & 0 & 1/\rho \\ \lambda + 2\mu & 0 & 0 & 0 & 0 \\ \lambda & 0 & 0 & 0 & 0 \\ 0 & \mu & 0 & 0 & 0 \end{bmatrix} \quad (7)$$

and

$$\mathbf{B} = \begin{bmatrix} 0 & 0 & 0 & 0 & 1/(\rho r) \\ 0 & 0 & 0 & 1/(\rho r) & 0 \\ 0 & \lambda/r & 0 & 0 & 0 \\ 0 & (\lambda + 2\mu)/r & 0 & 0 & 0 \\ \mu/r & 0 & 0 & 0 & 0 \end{bmatrix} \quad (8)$$

The numerical algorithm solves equation (6) with appropriate boundary condition at  $r = a$  and at  $r = b$ .

### Solution Scheme

As mentioned above, the numerical algorithm solves equation (2) or equation (6) with free surface or rigid boundary conditions at  $r = a$  (see figure 2) and with absorbing boundary conditions at the edges of the grid, at  $r = b$ . The variables are discretized on a spatial grid which is non uniform in the  $r$  direction and uniform in the  $\theta$  variable (Figure 1).

Equations (2) and (6) contains both spatial and temporal derivatives. For the  $r$  direction derivative we use a discrete Chebychev expansion:

$$\frac{\partial f(\bar{r}_j)}{\partial \bar{r}} = \sum_{k=0}^N b_k T_k(\bar{r}_j) \quad j = 0, \dots, N, \quad (9)$$

where  $N_r+1$  is the number of grid points in the  $r$  direction,  $-1 \leq \bar{r}_j \leq 1$  is the  $j^{\text{th}}$  sampling point in that direction,  $T_k$  are the discrete Chebychev polynomials, and the coefficients  $b_k$  are given by the recursion relation:

$$b_{k-1} = b_{k+1} + 2ka_k \quad k = N_r, \dots, 2 \quad (10)$$

$$\text{where } b_0 = \frac{2a_1 + b_2}{2}$$

(Gottlieb and Orszag 1977, Kosloff et. al. 1990).  $a_k$  are the coefficients of the discrete expansion of the original function, according to

$$f(\bar{r}_j) = \sum_{k=0}^N a_k T_k(\bar{r}_j) \quad (11)$$

(Hamming, 1978).

In actual applications the  $\bar{r}$  coordinate is related to the radius  $r$  by  $r = a + \frac{1}{2}(\bar{r}+1)(b-a)$ . Therefore,

$$\frac{\partial f}{\partial r} = \frac{\partial f}{\partial \bar{r}} \cdot \frac{2}{(b-a)}$$

For the  $\theta$  direction derivative we use the Fourier transform property:

$$\frac{df}{d\theta} \rightarrow iK_\theta \tilde{f} \quad (12)$$

where  $\tilde{f}$  is the Fourier transform of  $f$  and  $i$  is  $\sqrt{-1}$  (Bracewell 1978). The wave number  $K_\theta$  is given by:

$$K_\theta = j-1, \quad j = 1, \dots, N_\theta \quad (13)$$

where  $N_\theta$  is the number of grid points in the azimuthal direction. For advancing the solution in time we use a fourth order Runge-Kutta method.

### Boundary Conditions for the Acoustic Case

Three different types of boundary conditions are applied at the boundaries of the numerical grid. The free surface or rigid boundary condition is applied at  $r = a$  (figure 2) and the absorbing boundary condition is applied on the edges of the grid, at  $r = b$ . The appropriate boundary condition is achieved by setting the correct characteristic variables (Gottlieb et. al. 1982, Baylis et. al. 1986, Kosloff et. al. 1990). This process is based only on considering wave motion in the direction normal to the boundary, which in this case is the radial direction (Baylis et. al., 1986). At  $r = b$  we apply an absorbing boundary condition. We set the characteristic variable describing motion propagating outwards to remain constant and setting to zero the characteristic variable describing motion propagating into the grid according to:

$$\dot{P}^{(old)} - \frac{c}{r} \left[ r \frac{\partial P^{(old)}}{\partial r} \right] = \dot{P}^{(new)} - \frac{c}{r} \left[ r \frac{\partial P^{(new)}}{\partial r} \right] \quad (14)$$

$$0 = \dot{P}^{(new)} + \frac{c}{r} \left[ r \frac{\partial P^{(new)}}{\partial r} \right]$$

where  $(old)$  and  $(new)$  respectively, denote values of variables before and after application of the boundary condition. At  $r = a$  we apply either a free surface boundary condition or a rigid boundary condition. For the free surface boundary condition we retain the characteristic variable describing a wavelet that propagates towards the origin constant and zero the pressure field. This gives:

$$\dot{P}^{(old)} + \frac{c}{r} \left[ r \frac{\partial P^{(old)}}{\partial r} \right] = \dot{P}^{(new)} + \frac{c}{r} \left[ r \frac{\partial P^{(new)}}{\partial r} \right] \quad (15)$$

$$0 = \dot{P}^{(new)}$$

### Boundary Conditions for the Elastic Case

As in the acoustic case, absorbing boundary conditions are achieved by setting the correct characteristic variables. The rigid boundary condition at  $r = a$  requires zero values for  $U_r$  and for  $U_\theta$ . Keeping outgoing characteristic variables unmodified after application of the boundary condition implies,

$$\frac{1}{\rho V_s} \sigma_{\theta\theta}^{(new)} = \dot{U}_\theta^{(old)} + \frac{1}{\rho V_s} \sigma_{\theta\theta}^{(old)} \quad (16)$$

$$\frac{1}{\rho V_p} \sigma_{rr}^{(new)} = \dot{U}_r^{(old)} + \frac{1}{\rho V_p} \sigma_{rr}^{(old)}$$

$$\sigma_{\theta\theta}^{(new)} = \sigma_{\theta\theta}^{(old)} + \frac{\lambda}{\lambda+2\mu} \left[ \sigma_{rr}^{(new)} - \sigma_{rr}^{(old)} \right]$$

where  $V_p$  and  $V_s$  are respectively P and S waves velocity. At  $r = b$  we use the absorbing condition which yields,

$$\sigma_{\theta\theta}^{(new)} = \frac{1}{2} \left[ \sigma_{\theta\theta}^{(old)} - \rho V_s \dot{U}_\theta^{(old)} \right] \quad (17)$$

$$\dot{U}_\theta^{(new)} = \frac{1}{2} \left[ \dot{U}_\theta^{(old)} - \frac{1}{\rho V_s} \sigma_{\theta\theta}^{(old)} \right]$$

$$\sigma_{rr}^{(new)} = \frac{1}{2} \left[ \sigma_{rr}^{(old)} - \rho V_p \dot{U}_r^{(old)} \right]$$

$$\dot{U}_r^{(new)} = \frac{1}{2} \left[ \dot{U}_r^{(old)} - \frac{1}{\rho V_p} \sigma_{rr}^{(old)} \right]$$

$$\sigma_{\theta\theta}^{(new)} = \sigma_{\theta\theta}^{(old)} + \left[ \sigma_{rr}^{(new)} - \sigma_{rr}^{(old)} \right] \frac{\lambda}{\lambda + 2\mu}$$

**Example - Scattering by a Cylindrical Object**

We set  $r = a$  (figure 2) to be 80 meters and we locate a source with hightcut frequency of 40 Hz on the horizontal ( $\theta = 0$ ), at a distance of 170 m from the origin (Figure 3). Three receivers are situated at different locations. Receiver A is located 200 m to the right of the source, receiver B at a distance of 370 m from the center and at an azimuthal angle of 15 degrees, and receiver C is located at a distance of 450 m from the center and at an azimuthal angle of 30 degrees. Figures 4a, 4b, 4c and 4d show the pressure wave field at times 0.1 sec, 0.2 sec, 0.3 sec and 0.4 sec, respectively. We can see the direct wave and the partition of energy by the circular object. Part of the energy is reflected and part crawls along the cylindrical interface. Figures 5a and 5b show the time history seismograms that were recorded at receivers B and C, respectively. The continuous line represents the numerical result; the dots are the analytical result. We also locate two receivers on the surface of the cylindrical object, on  $r = a$ . The first receiver is located at an azimuthal angle of zero degrees, and the second one at an angle of 15 degrees. Figures 6a and 6b shows respectively the time history seismograms that was recorded at an angle of zero degrees and at an angle of 15 degrees. Again, the continuous line gives the numerical result while the dots are the analytical results.

**References**

A. Baylis, K.E. Jordan, B.J. LeMesurier & E. Turkel, A forth-order accurate finite-difference scheme for the computation of elastic waves, Bulletin of the seismological society of america, Vol. 76, No. 4, 1986.

Bracewell, The Fourier transform and its applications, McGraw Hill book company, 1978.

J. Gazdag, Modeling of the acoustic wave equation with transform methods, Geophysics, vol. 46, 1981.

Y. C. Fung, Foundations of Solid Mechanics, McGraw-Hill book company, 1965.

D. Gottlieb, M. Gunzburger & E. Turkel, On numerical boundary treatment of hyperbolic systems for finite difference and finite element methods, SIAM J. Numer. Anal., Vol. 19, No. 4, 1982.

D. Gottlieb and S. Orszag, Numerical analysis of spectral methods, theory and applications. Society for industrial and applied mathematics, 1977.

R. Hamming, Numerical methods for scientists and engineers, McGraw- Hill book company, 1978.

D. Kosloff & E. Baysal, Forward modeling by a Fourier method, Geophysics, vol. 47, 1402-1412, 1982.

D. Kosloff, D. Kessler, A.Q. Filho, E. Tessmer, A. Behle & R. Strahilevitz, Solutions of the equations of dynamic elasticity by a Chebychev spectral method, Geophysics, summer 1990.

D. Kosloff, H. Tal-Ezer, Modified Chebychev pseudospectral method with  $O(N^{-1})$  time step restriction, submitted to Jour. of Numerical Physics, 1989.

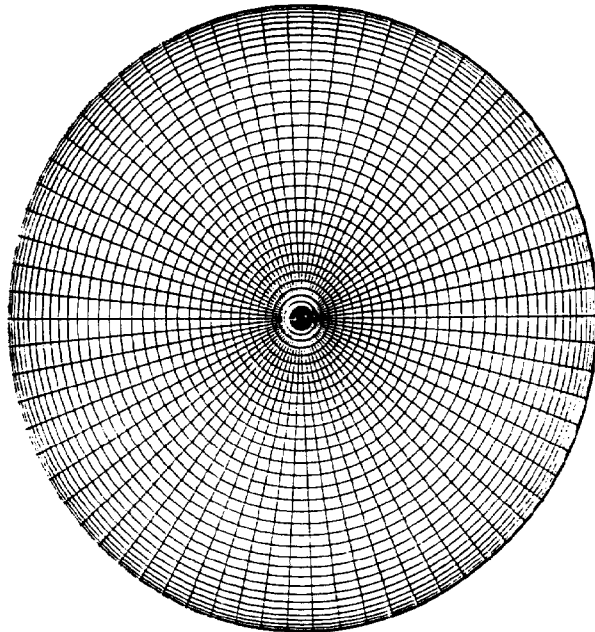


Figure 1: Chebychev-Fourier numerical grid. number of  $\theta$  grid points is 70.

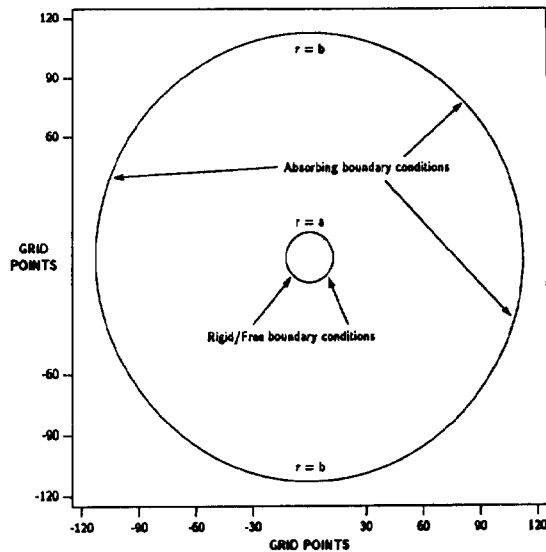


Figure 2: Configuration of boundary conditions.

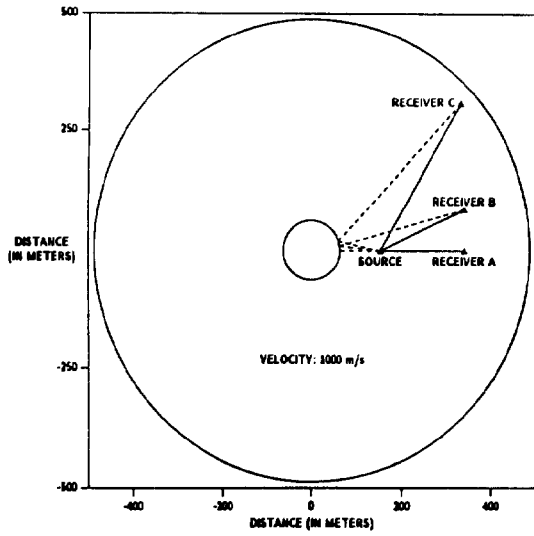


Figure 3: Scattering by a cylindrical object. Continuous lines are direct waves paths and broken lines are reflected waves paths.

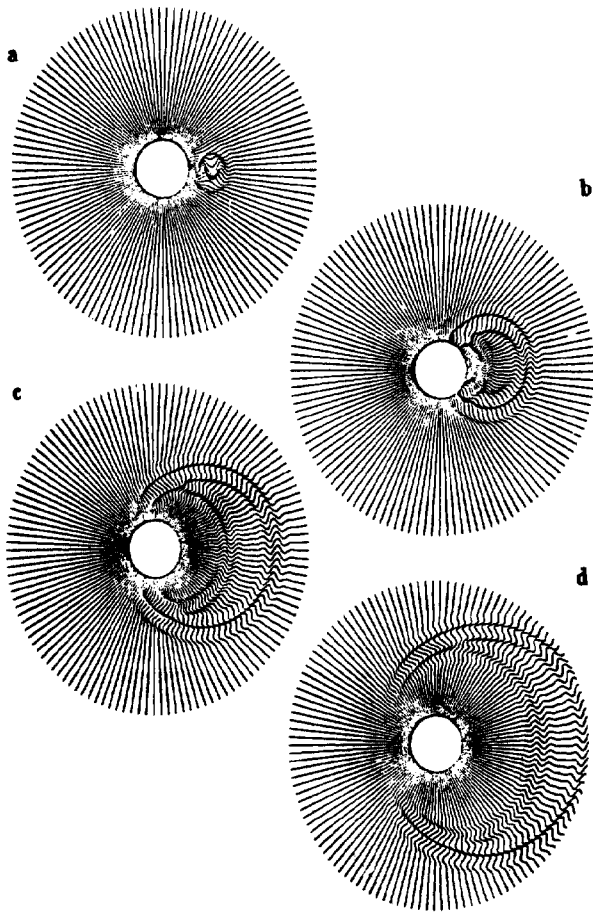


Figure 4: Scattering by a cylindrical object. Pressure snapshot at time 0.1, 0.2, 0.3 and 0.4 s.

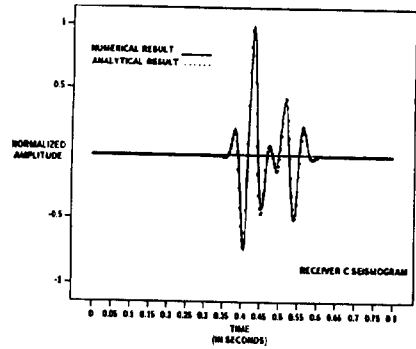
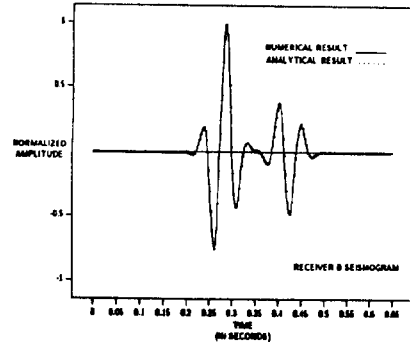


Figure 5: Seismograms recorded by receivers B and C.

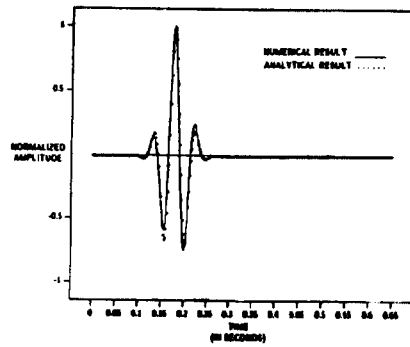
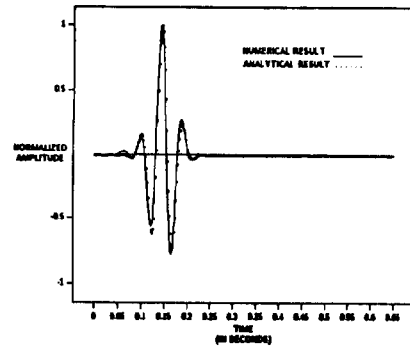


Figure 6: Seismograms recorded on the cylindrical surface.